Reactivity of Deprotonated $Mn_2(\mu$-H)$(\mu$-PCyH)$(CO)_8$: Valence Isomerization and Rearrangement of $Mn_2(AuPR_3)_2(\mu_4$-PCy)$(CO)_8$ and $Mn_2(\mu$-$AuPR_3)(\mu_3$-PCy$(AuPR_3))(CO)_8$ (R = Ph, p-C_6H_4F, p-C_6H_4OMe, Cy, Et, $(CH_2)_2CN$)

H.-J. Haupt,* M. Schwefer, and U. Flörke

Department of Inorganic and Analytical Chemistry, Universität-GH Paderborn, 33098 Paderborn, FRG

Received April 29, 1994[⊗]

In THF solution the dimanganese complex $Mn_2(\mu$-H)$(\mu$-PCyH)$(CO)_8$ (**1**) is deprotonated by excess DBU (1,8-diazabicyclo[5.4.0]undecen-7-en) to an anionic species which on addition of 2 equiv of $ClAuPPh_3$ at 20 °C in 1 h gives the isomers $Mn_2(AuPPh_3)_2(\mu_4$-PCy$)(CO)_8$ (**2**) and $Mn_2(\mu$-$AuPPh_3)(\mu_3$-PCy$(AuPPh_3))(CO)_8$ (**3**). From the dissolved mixture of isomers the thermodynamically more preferred isomer **2** was crystallized and identified by a single crystal X-ray analysis, whereas **3** was characterized by ^{31}P NMR data. A solution of **2** gives rise to an equilibrium mixture of **2** and **3** in the chosen solvents. The factors influencing the equilibrium position for the enantiotropically convertible μ_3/μ_4-bridged isomers were determined by ^{31}P NMR measurements. The variation of the reagent $ClAuPR_3$ with R = Ph, p-C_6H_4OMe, p-C_6H_4F, Cy, Et, and $(CH_2)_2CN$ and the solvent in the aforementioned reaction system showed that the equilibrium between the isomers $Mn_2(AuPR_3)_2(\mu_4$-PCy$)(CO)_8$/ $Mn_2(\mu$-$AuPR_3)(\mu_3$-PCy$(AuPR_3))(CO)_8$ depends on electronic and/or steric factors and on the polarity of the solvent. The μ_3-bridged isomer **3** is favored by a −I effect of the R groups, and the μ_4-bridged isomer **2** by a +M effect of such groups. In spite of the +I effect of Cy in PCy_3 it was possible to separate a μ_3-bridged isomer, Mn_2-$(\mu$-$AuPCy_3)(\mu_3$-PCy$(AuPCy_3))(CO)_8$ (**5**), due to a bigger steric strain in the related (μ_4-P) bridged isomer. The molecular structure of **5** was ascertained by an X-ray analysis. The structure of **5** can be derived from **1** by the exchange of both hydrogen atoms for $AuPCy_3$ groups as substituents. The molecular structure shows a typical edge-sharing coordination bioctahedron with a Mn−Mn bond length of 3.041(2) Å. From **5** to the other isomer **2** one of the Au−Mn bonds converts to an Au−Au bond and the additional generation of an Au−P bond leads to a μ_4-bridged P atom. Combined with these alterations the strongly distorted $Mn_2Au_2(\mu_4$-P) core is formed which has trans-positioned an opened and closed Mn−Au edge. The inequivalence of the edges of **2** in the solid disappears in solution. On the time scale of the ^{31}P NMR method there are two fluxional Mn−Au bonds in the course of a topomerization process. To our knowledge, this is the first example of a permanent valence isomerization of heterometallic bonds in a cluster compound. This and other features of the complex reaction system are discussed.

Introduction

Recently, we described deprotonation reactions of hydrido diorganophosphido-bridged dimanganese/(di)rhenium carbonyl complexes to generate anionic intermediates for directed cluster expansion.[1-4] In continuation of these studies with metal−metal-bonded anions, we here report on our efforts to achieve a successive hydrogen substitution in the bifunctional $Mn_2(\mu$-H$)(\mu$-PCyH$)(CO)_8$ (**1**). Such attempts are valuable for systematic syntheses of small heterometallic cluster compounds in good yields. Furthermore, they are of special interest in the investigation of chiral metal cores and, finally, of their catalytic ability.[5]

Experimental Section

Infrared spectra were run for the 2200−1600 cm^{-1} metal carbonyl region in CH_2Cl_2 and recorded on a Nicolet P510 FTIR spectrometer. Proton NMR and phosphorus-31 NMR spectra were taken on a Bruker AMX 300 multinuclear pulsed Fourier transform spectrometer at 300 and 121.5 MHz, respectively, using internal tetramethylsilane and external 85% phosphoric acid, respectively, as a reference. Chemical shifts are given in ppm downfield from the reference. All reactions were carried out under an argon atmosphere. Tetrahydrofuran and xylene were dried according to literature methods and distilled and stored in the presence of argon. The gold complexes $ClAuPR_3$ (R = Ph, p-C_6H_4F, p-C_6H_4OMe, Cy, Et, $(CH_2)_2CN$) were prepared according to the cited published procedure.[6]

Preparation of $Mn_2(\mu$-H$)(\mu$-PCyH$)(CO)_8$ (1). A 335 mg amount of $Mn_2(CO)_{10}$ (0.86 mmol) was heated with 100 μL of H_2PCy (0.86 mmol) in xylene solution at 170 °C for 18 h in a sealed glass tube. After cooling the glass tube was opened, the solvent removed under reduced pressure, and the residue obtained separated by use of TLC (PSC plate, silica 60, Fa. Merck) with n-hexane as eluant. The chromatogram contained two yellow fractions: (1) (higher R_f value) $Mn_2(CO)_{10}$; (2) $Mn_2(\mu$-H$)(\mu$-PCyH$)(CO)_8$ and *cis*- and *trans*-$Mn_2(\mu$-$PCyH)_2(CO)_8$. After isolation fraction 2 was stirred in 12 mL of methanol for 1 h at room temperature. The solution was then filtered to separate a light yellow precipitate of $Mn_2(\mu$-$PCyH)_2(CO)_8$. The filtrate was evaporated to dryness, and **1** remained as a dark yellow solid. Yield: 158 mg of **1** (40.8%) and 51 mg of *cis*- and *trans*-Mn_2-$(\mu$-$PCyH)_2(CO)_8$ (10.5%). Fractional crystallization of *cis*- and *trans*-$Mn_2(\mu$-$PCyH)_2(CO)_8$ by a repeated application of the vapor diffusion method from CH_2Cl_2 in the presence of n-pentane enabled the separation of the cis and trans isomers.[7]

⊗ Abstract published in *Advance ACS Abstracts,* December 1, 1994.

(1) Haupt, H.-J.; Heinekamp, C.; Flörke, U. *Inorg. Chem.* **1990**, *29*, 2955.
(2) Haupt, H.-J.; Flörke, U.; Disse, G.; Heinekamp, C. *Chem. Ber.* **1991**, *124*, 2191.
(3) Haupt, H.-J.; Heinekamp, C.; Flörke,U.; Jüptner, U. *Z. Anorg. Allg. Chem.* **1992**, *608*, 100.
(4) Haupt, H.-J.; Merla, A.; Flörke, U. Z. *Anorg. Allg. Chem.* **1994**, *620*, 999.
(5) Gladfelter, W. L.; Rosselet, K. J. *Cluster Complexes as Homogeneous Catalysts and Catalyst precursor in Chemistry of Metal Cluster Complexes*; Shriver, D. F., Kaesz, H. D., Adams, R. D., Eds.; VCH Publisher Inc.: New York, 1990.
(6) Brauer, G. *Handbook of Preparative Inorganic Chemistry*; F. Enke Verlag: Stuttgart, 1981; Volume 3.

0020-1669/95/1334-0292$09.00/0

1. Anal. Calcd for $C_{14}H_{13}Mn_2O_8P$ (M_r = 450.10): C, 37.36; H, 2.91. Found: C, 37.51; H, 2.95. IR (CH_2Cl_2) (cm^{-1}): ν_{CO} 2093 w, 2060 m, 2000 vs, 1966 s. ^1H NMR ($CDCl_3$): δ −17.34 (d; $^2J(PH)$ = 33 Hz; 1H, μ-H); 1.3−2.3 (m; 11 H, Cy); 4.21 (dd; $^1J(PH)$ = 327 Hz; $^3J(HH(Cy)$ = 9 Hz; 1H, μ-PH). ^{31}P NMR($CDCl_3$): δ 103.2 (s; 1P, μ-PCyH); hydrogen-coupled, δ 103.4 (d; $^1J(PH)$ = 329 Hz; 1P, μ-PCyH).

***cis*-$Mn_2(\mu$-PCyH$)_2(CO)_8$.** Anal. Calcd for $C_{20}H_{24}Mn_2O_8P_2$ (M_r = 564.23): C, 42.57; H, 4.29. Found: C, 41.94; H, 4.80. IR (cyclopentane) (cm^{-1}): ν_{CO} 2049 m, 1999 vs, 1981 vs, 1968 m. ^1H NMR ($CDCl_3$): δ 1.0−2.2 (m); 2.21 (s); 2.53 (dd; $^1J(PH)$ = 290 Hz; $^3J(HH-(Cy))$ = 8 Hz); 2.85 (s); 3.23 (s). ^{31}P NMR ($CDCl_3$): δ −88 (s; 2P, μ-PCyH) [broad].

***trans*-$Mn_2(\mu$-PCyH$)_2(CO)_8$.** Anal. Calcd for $C_{20}H_{24}Mn_2O_8P_2$ (M_r = 564.23): C, 42.57; H, 4.29. Found: C, 42.34; H, 4.43. IR (cyclopentane) (cm^{-1}): ν_{CO} 2049 m, 1987 vs, 1964 s. ^1H NMR ($CDCl_3$): δ 1.1−2.2 (m); 2.32 (s); 2.63 (dd; $^1J(PH)$ = 286 Hz; $^3J(HH-(Cy))$ = 6 Hz); 2.95 (s); 3.35 (s). ^{31}P NMR ($CDCl_3$): δ −88 (s; 2P, μ-PCyH) [broad].

The ^1H NMR spectra of *cis*- and *trans*-$Mn_2(\mu$-PCyH$)_2(CO)_8$ in $CDCl_3$ solution in the PCyH region are second-order AA'XX' spectra.[8] In addition to the sharp double doublets in each case three singlets were recorded due to two AB subspectra.. The fourth signal is hidden under the multiplet of the cyclohexyl protons. A splitting of the subspectra by coupling to the *o*-protons of the cyclohexyl groups was not resolved.

Preparation of $Mn_2(AuPPh_3)_2(\mu_4$-PCy$)(CO)_8$ (2) and $Mn_2(\mu$-AuPPh$_3)(\mu_3$-PCy(AuPPh$_3$))$(CO)_8$ (3). A solution of 100 mg of $Mn_2(\mu$-H)$(\mu$-PCyH$)(CO)_8$ (0.22 mmol) and 100 μL of DBU (0.68 mmol) in 10 mL of THF was stirred for 1 h at room temperature. After addition of 250 mg of $ClAuPPh_3$ (0.51 mmol) the solution turned dark red. The solution was then stirred for one more hour and subsequently evaporated to dryness. The red residue obtained was purified by TLC with CH_2Cl_2/*n*-hexane (1:2) as eluant. Yield: 282 mg of **2/3** (95.3%).

2/3. Anal. Calcd for $C_{50}H_{41}Au_2Mn_2O_8P_3$ (M_r = 1366.60): C, 43.94; H, 3.02. Found: C, 43.54; H, 3.15. IR (CH_2Cl_2) (cm^{-1}): ν_{CO} 2039 m, 2004 m, 1985 m, 1964 s, 1950 vs, 1928 m (sh), 1909 m, 1893 w (sh). ^1H NMR ($CDCl_3$): δ 1.3−2.4 (m; 11H, Cy); 7.3−7.6 (m; 30H,-Ph). ^{31}P NMR ($CDCl_3$): δ 45.1 (d; $^2J(PP)$ = 273 Hz; 1P); 47.0 (d; $^2J(PP)$ = 154 Hz; 2P); 62.8 (s; 1P); 81.2 (t; $^2J(PP)$ = 155 Hz; 1P); 223.1 (d; $^2J(PP)$ = 273 Hz; 1P).

In accord with this synthesis the analogous mixtures of isomers $Mn_2(AuPR_3)_2(\mu_4$-PCy$)(CO)_8/Mn_2(\mu$-AuPR$_3)(\mu_3$-PCy(AuPR$_3$))$(CO)_8$ (R = *p*-C_6H_4F, *p*-C_6H_4OMe, Cy, Et, $(CH_2)_2CN$) were generated by treatment of $Mn_2(\mu$-H$)(\mu$-PCyH$)(CO)_8$ with DBU and $ClAuPR_3$. The eluants used for purification by TLC are given as follows: R = Ph, CH_2Cl_2/*n*-hexane (1:2); R = *p*-C_6H_4F, CH_2Cl_2/*n*-hexane (1:1); R = *p*-C_6H_4OMe, CH_2Cl_2; R = Cy, CH_2Cl_2/*n*-hexane (1:15); R = Et, CH_2Cl_2/*n*-hexane (1:15); R = $(CH_2)_2CN$, ethyl acetate. All the new compounds gave satisfactory elemental analysis.

^{31}P NMR data of the analogous mixture of isomers $Mn_2(\mu$-AuPPh$_3)(\mu$-PCy(AuPPh$_3$))$(CO)_8/Mn_2(AuPR_3)_2(\mu_4$-PCy$)(CO)_8$ (R = *p*-C_6H_4F, *p*-C_6H_4OMe, Cy, Et, $(CH_2)_2CN$) recorded in DMSO are as follows: R = Ph: 224.4 (d, 272); 82.5 (t, 157), 62.8 (s); 47.2 (d, 157); 45.3 (d, 272). R = *p*-C_6H_4F: 224.9 (d, 275); 82.2 (t, 156); 61.1 (s); 45.1 (d, 156); 43.7 (d, 275). R = *p*-C_6H_4OMe: 224.7 (d, 281); 83.0 (t, 161); 60.0 (s); 43.7 (d, 161); 42.1 (d, 281). R = Cy: 231.8 (d, 261); 81.3 (t, 151); 80.6 (s); 64.7 (d, 151); 63.6 (d, 263). R = Et: 232.3 (d, 276); 88.8 (t, 154); 65.7 (s); 49.4 (d, 277); 49.4 (d, 157). R = $(CH_2)_2$-CN: 230.0 (d, 275); 83.9 (t, 143); 61.0 (s); 43.4 (d, 275); 42.9 (d, 143).

Structure Determination of 2 (Figure 3). Lattice parameters were refined from 28 reflections with $12 \le 2\theta \le 32°$. Data were collected on a Siemens R3m/V diffractometer, with $\omega/2\theta$ scan, $3 \le 2\theta \le 52°$, 10 203 intensities, 3 standards recorded every 400, 6% decay, and intensities corrected accordingly. *Lp* and empirical absorption corrections (ψ scans) were performed, and after merging (R_{int} = 0.035) 6381 unique observed intensities were observed with $F > 4\sigma(F)$. The structure was solved by direct and conventional Fourier methods. Full-matrix least-squares refinement was based on F and 514 parameters, with all but H-atoms refined anisotropically, phenyl groups treated as rigid bodies (C−C = 1.395 Å), and H-atoms fixed at idealized positions. The residuals were in the final ΔF map of −0.83/1.25 e/Å^3 near the Au position. Further information is given in Table 2 Scattering factors, structure solution, and refinement were determined with SHELXTL-Plus.[9] Other programs: PARST,[10] MISSYM.[11]

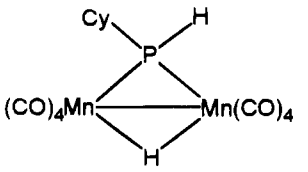

Figure 1. Structural diagram for $Mn_2(\mu$-H$)(\mu$-PCyH$)(CO)_8$ (**1**).

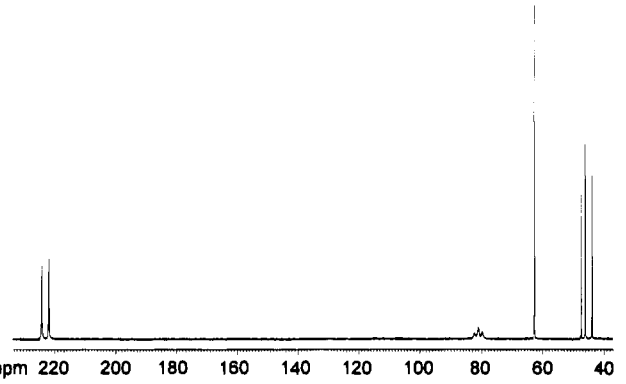

Figure 2. ^{31}P NMR spectrum of isomers **2** and **3** in $CDCl_3$ solution at 298 K. See text for discussion of resonances.

Structure Determination of 5 (Figure 7). Lattice parameters were refined from 25 reflections with $14 \le 2\theta \le 30°$. Data were collected with an $\omega/2\theta$ scan, $5 \le 2\theta \le 55°$, and 13 305 intensities. Standards were as before, with only random deviations. Corrections and structure solution were as before. A total of 12 927 independent reflections (R_{int} = 0.039) were obtained. Refinement was based on F^2 and 586 parameters, with all but H-atoms refined anisotropically. Residuals in final ΔF map: −0.82/1.17 e/Å^3. Scattering factors and structure refinement: SHELXL-93.[12] Other programs were as before.

Results and Discussion

To achieve the desired substitution of two hydrogen atoms in $Mn_2(\mu$-H$)(\mu$-PCyH$)(CO)_8$ (**1**) (Figure 1) whose structure is known from a single crystal X-ray analysis,[13] an isolobal exchange of a proton H^+ for a cationic group $AuPPh_3^+$ must be possible twice. For this purpose the yellow compound **1** which was obtained by the reaction of equimolar amounts of $Mn_2(CO)_{10}$ and H_2PCy in xylene solution at 170 °C for 18 h in a sealed glass tube was deprotonated by an excess of the base DBU in THF solution at 20 °C for 1 h. With 2 equiv of $ClAuPPh_3$ the anionic intermediate gave a red solid (yield 95%) of the formula-like composition $C_{50}H_{41}Au_2Mn_2O_8P_3$. The purity of the product was ascertained by the result of an elemental analysis and the correct integral ratio of ^1H NMR signals for protons in the groups Cy/3Ph (11/30). The ^{31}P NMR spectrum of the product in $CDCl_3$ solution (Figure 2) shows a complex pattern indicating a mixture of isomers which could not be separated by the TLC procedure used. However, it was possible to crystallize one of the isomers by application of the vapor pressure equilibration method. The molecular structure of this

(7) Flörke, U; Haupt, H.-J. *Acta Crystallogr.* **1993**, *C48*, 374.
(8) Brown, M. P.; Buckett, J.; Harding, M. M.; Lynden-Bell, R. M.; Mays, M. J.; Woulfe, K. W. *J. Chem. Soc., Dalton Trans.* **1991**, 3097.
(9) Sheldrick, G. M. SHELXTL-Plus. Siemens Analytical X-ray Instruments Inc., Madison, WI, 1991.
(10) Nardelli, M. *Comput. Chem.* **1983**, *7*, 95.
(11) LePage, Y. *J. Appl. Crystallogr.* **1987**, *20*, 264.
(12) Sheldrick, G. M. SHELXL-93. Program for Crystal Structure Refinement. Univ. of Göttingen, Germany, 1993.
(13) Flörke, U.; Haupt H-.J. *Z. Kristall.*, in press.

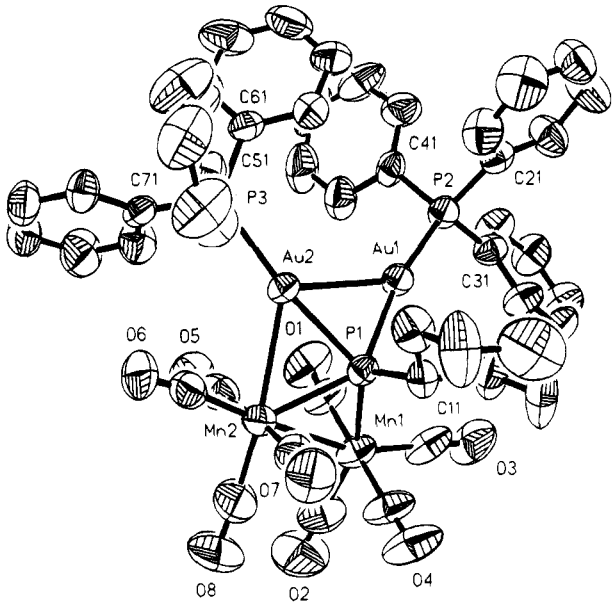

Figure 3. Molecular structure of $Mn_2(AuPPh_3)_2(\mu_4\text{-}PCy)(CO)_8$ (**2**). Hydrogen atoms are omitted. The ORTEP plot shows 50% probability for thermal ellipsoids.

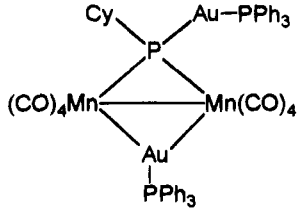

Figure 4. Structural diagram for $Mn_2(\mu\text{-}AuPPh_3)(\mu_3\text{-}PCy(AuPPh_3))(CO)_8$ (**3**).

isomer $Mn_2(AuPPh_3)_2(\mu_4\text{-}PCy)(CO)_8$ (**2**) is given in Figure 3. Hence the other isomer must be the compound $Mn_2(\mu\text{-}AuPPh_3)(\mu_3\text{-}PCy(AuPPh_3))(CO)_8$ (**3**) (Figure 4). This conclusion for **3** is proved by the ^{31}P NMR data in Figure 2 as follows: 45.1 ppm (d,^2J(PP) 273 Hz, 1P, PPh_3), 62.8 ppm (s, 1P, PPh_3), and 223.1 ppm (d, ^2J(PP) 273 Hz, 1P, μ-P). But it was difficult to assign the remaining ^{31}P NMR data to **2**, because the molecular solid state structure of **2** with three chemically inequivalent phosphorus atoms demands three double doublets. Instead of such signal groups, the ^{31}P NMR pattern shows a triplet at 81.2 ppm (155 Hz) and a doublet at 47.0 ppm (154 Hz). To correlate the experimental data with the given theoretical demand, it must be assumed that the isomer **2** undergoes a permanent (reversible) valence isomerization process which, in this case, is equivalent to a racemization process. Thus both P ligand atoms of the PPh_3 groups appear as chemically equivalent within the time scale of ^{31}P NMR measurements. Consequently, the signal of the μ_4-P ligand atom is a triplet. Its position is relatively high-field shifted. This can be explained as being due to a reduced metal−metal bond order in **2** as compared to that of the solvated species **3**. The above NMR data for **2** are as expected for the transition state of a valence isomerization process. The reaction can be classified as topomerization (fluxional process) which is based on a degenerate valence isomerization (Figure 5). The fluxional behavior of the related inorganic Mn_2Au_2 metallacycle is analogous to that of homoaromatics like bullvalene or semibullvalene.[14] This view is supported by a very low activation energy of the valence isomerization of **2**, because a low-temperature ^{31}P NMR measurement at −70 °C showed no

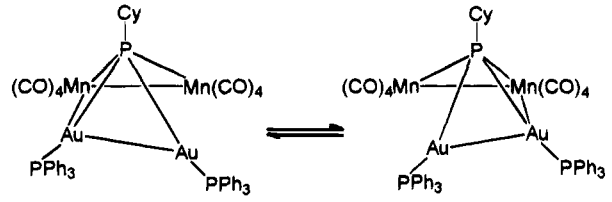

Figure 5. Valence isomerization of $Mn_2(AuPPh_3)_2(\mu_4\text{-}PCy)(CO)_8$ (**2**).

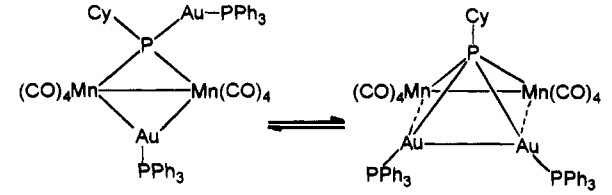

Figure 6. Isomerization of $Mn_2(\mu\text{-}AuPPh_3)(\mu_3\text{-}PCy(AuPPh_3))(CO)_8$ (**2**) and $Mn_2(AuPPh_3)_2(\mu_4\text{-}PCy)(CO)_8$ (**3**).

alteration of the two groups of signals required in accordance with the equilibrium in Figure 5. Further cooling of the sample led to crystallization of **2**. A similar behavior of a homo- rather than a heterometallic metallacycle is known for $Re_4(\mu\text{-}Cl)_2(\mu\text{-}PPh_2)_4(\mu_4\text{-}PPh)(CO)_8$, which has three Re−Re bonds and one nonbonding Re···Re contact length in the solid. The ^{31}P NMR spectrum of this rhenium cluster complex in $CDCl_3$ solution shows only three groups of signals (223.3 ppm (t; 2P); −8.2 ppm (t; 1P); −109.7 ppm (dt; 2P)) instead of four groups of signals as required for the molecular solid state structure. A low-temperature measurement provided no change in the described pattern. This means that a spectroscopic equivalence of both diametrically positioned μ-PPh_2 groups is responsible for a permanent valence isomerization process in the homometallic core.[15] To our knowledge, **2** is the first example showing such a process in a heterometallic core.

Complete crystallization of the solution of both the isomers **2** and **3** gave only dark red crystals of **2** which was proved by Guinier powder patterns. This observation corresponds to an one-sided isomerization process from **3** to **2**. To verify an enantiotropic process (Figure 6), it has to be shown that the reciprocal process for **2** takes place on dissolving the crystals. This was done, for example, in $CDCl_3$ and revealed that the isomers **2/3** are again present in a ratio of 74/26 as in Figure 2.

As a next step the dependency of this reversible isomerization process (Figure 6) on the nature of the phosphine ligand attached to Au was investigated in different solvents. For this purpose, **1** was treated with excess DBU and 2 equiv of $ClAuPR_3$ (R = Ph, p-C_6H_4OMe, p-C_6H_4F, Cy, Et, $(CH_2)_2CN$) to provide the relevant mixture of μ_3/μ_4-bridged isomers under the reaction conditions used previously. The ratio of the isomer pairs in the various solvents was determined by ^{31}P NMR measurements (pulse 3 μs, 38°). The equilibrium state was achieved immediately after dissolving the respective mixtures of isomers. ^{31}P NMR spectra of **2/3** remained unchanged in the course of time as well as all other mixtures $Mn_2(\mu\text{-}AuPR_3)(\mu_3\text{-}PCy(AuPR_3))(CO)_8/Mn_2(AuPR_3)_2(\mu_4\text{-}PCy)(CO)_8$ (R = p-C_6H_4F, p-C_6H_4OMe, Cy, Et, $(CH_2)_2CN$) showed no more temporal alteration. The particular ratios μ_3/μ_4 were obtained by evaluation of the intensity of each PR_3 resonance signal. It can be assumed that there is no falsification of the μ_3/μ_4 ratio determined as being due to potential difference between ^{31}P T_1 values for the PR_3 groups in the μ_3 and μ_4 isomers within the exactness of the values given. This presumption is not

(14) Paquette, L. *Top. Curr. Chem.* **1984**, *119*, 58.

(15) Klouras, N.; Flörke, U.; Haupt, H.-J.; Woyciechowski, M. *Acta Crystallogr.* **1990**, *C46*, 2096.

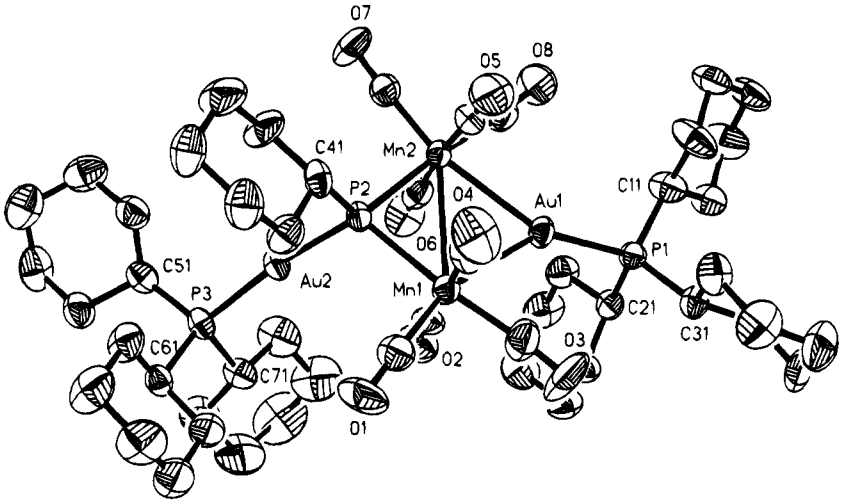

Figure 7. Molecular structure of $Mn_2(\mu\text{-AuPCy}_3)(\mu_3\text{-PCy(AuPCy}_3))(CO)_8$ (**5**). Hydrogen atoms are omitted. The ORTEP plot shows 50% probability for thermal ellipsoids.

Table 1. Ratio of $Mn_2(\mu\text{-AuPR}_3)(\mu_3\text{-PCy(AuPR}_3))(CO)_8$ and $Mn_2(AuPR_3)_2(\mu_4\text{-PCy})(CO)_8$ in Selected Solvents (Solvent Polarity According to Hildebrand's Scale)

	$Mn_2(\mu\text{-AuPR}_3)(\mu_3\text{-PCy(AuPR}_3))(CO)_8/Mn_2(AuPR_3)_2(\mu_4\text{-PCy})(CO)_8$			
R	C_6H_6 (0.32)	$CDCl_3$ (0.40)	CH_2Cl_2 (0.42)	DMSO (0.62)
Ph	86/14	74/26	41/59	11/89
p-C_6H_4F	97/3	92/8	74/26	10/90
p-C_6H_4OMe	74/26	58/42	34/66	8/92
Cy	99/1	91/9	79/21	37/63
Et	96/4	85/15	71/29	17/83
$(CH_2)_2CN$	insoluble	insoluble	98/2	87/13

unreasonable as the PR_3 groups which signals were integrated do not differ in their direct chemical environnment ($\Delta\delta$ < 5 ppm). In case of the related monoaurated complexes $Mn_2(\mu\text{-AuPR}_3)(\mu\text{-PCyH})(CO)_8$ and $Mn_2(\mu\text{-H})(\mu_3\text{-PCy(AuPR}_3))(CO)_8$ (R= Ph, Cy) the accuracy of the ^{31}P NMR method applied could be proved by UV/vis measurements.[16] The results are displayed in Table 1.

First, the results illustrate that the ratio of the μ_3/μ_4-bridged isomers is reduced by an increase of the solvent polarity independent of variation of the R residues. For the residue R = Ph in PR_3, for example, the ratio of μ_3/μ_4-bridged isomers changes from 86/14 in benzene to 11/89 in the polar dimethyl sulfoxide (DMSO). We suggest that the the observed equilibrium shift is due to a larger dipole of the μ_4-bridged isomer. This conclusion seems not unreasonable as the one-sided arrangement of the $AuPR_3$ groups in $Mn_2(AuPR_3)_2(\mu_4\text{-PCy})(CO)_8$ should bring about a larger permanent dipole than the diametric arrangement in the μ_3 isomer. Besides it should be more easy to polarize $Mn_2(AuPR_3)_2(\mu_4\text{-PCy})(CO)_8$ because of its permanent valence isomerization (induced dipole).

Second, the results in Table 1 are helpful in analyzing the influence of electronic factors on an equilibrium shift for the μ_3/μ_4-bridged isomers. Their ratio in the following series of sterically equivalent ligands PR_3 (R = Ph, *p*-C_6H_4F, *p*-C_6H_4-OMe) attached to gold(I) atoms depends only on the electronic properties of the particular R groups. Going from R = Ph to *p*-C_6H_4F, the −I effect of fluoro substituent increases the ratio of the μ_3/μ_4-bridged isomers, and in the other case from R = Ph to *p*-C_6H_4OMe, the +M effect decreases the observed ratio. These observations are valid in all the solvents used. Furthermore, the dependency of the isomer ratio on a −I effect is additionally confirmed by changing R from Et to $(CH_2)_2CN$: The ratio increases from 71/29 to 98/2 in CH_2Cl_2 and 17/83 to 87/13 in DMSO solution. The large sensitivity to the aforementioned solvent polarity and the electronic factors (−I and +M effects) has different origins. Whereas the equilibrium shift in the first case is controlled by solvation energy, it is based on an alteration of the kind of metal−metal bonds and the number of metal−ligand bonds in the second case.

Third, the results show the possibility of steric control for the particular equilibrium shifts. To prove this, the steric demanding ligand PCy_3 attached to gold(I) atoms was selected. For electronic reasons the ratio of the μ_3/μ_4-bridged isomers should be reduced going from R = Ph to Cy in the absence of a steric strain due to the bigger pk_a value of 9.70 for PCy_3 compared to that of 2.73 for PPh_3.[17] Actually, the steric hindrance between the two $AuPCy_3$ groups exceeds the electronic effect, so that the isomer ratio increases from 41/59 (R = Ph) to 79/21 (R = Cy) in CH_2Cl_2 solution. Finally, it remains to say that this steric strain opens the way to crystallization of the μ_3-isomer $Mn_2(\mu\text{-AuPCy}_3)(\mu_3\text{-PCy(AuPCy}_3))(CO)_8$ (Figure 7) by application of the vapor pressure equilibration method (CH_2Cl_2/*n*-pentane). To verify the dominance of steric strain as the factor influencing the observed equilibrium shift, a computer-assisted simulation based on the structural parameters of **2** when the ligands PPh_3 were replaced by PCy_3 was undertaken. It was shown that geometries without strong repulsive interactions were not possible, which supports the aforementioned considerations. The observed equilibrium shift is therefore caused by steric strain.

Fourth, the reagent $ClAuP(EtCN)_3$ bearing $P(EtCN)_3$ with a pk_a of 1.37 [17] in the previously mentioned reaction system combines an enhancement of an electronic factor as well as steric strain and, consequently, should give the μ_3-bridged isomer in excess. This demand is completely fulfilled, as the ratio of the

(16) Haupt, H.-J.; Schwefer, M.; Egold, H.; Flörke, U. *Inorg. Chem.*, submitted for publication.

(17) Streuli, C. A. *Anal. Chem.* **1960**, *32*, 985.

Table 2. Crystallographic Data for **2** and **5**

	$Mn_2(AuPPh_3)_2(\mu_4\text{-}PCy)(CO)_8$	$Mn_2(\mu\text{-}AuPCy_3)(\mu_3\text{-}PCy(AuPCy_3))(CO)_8$
formula	$Au_2C_{50}H_{41}Mn_2O_8P_3$	$Au_2C_{50}H_{77}Mn_2O_8P_3$
mol wt	1366.6	1402.8
cryst size, mm	0.09 × 0.30 × 0.51	0.22 × 0.32 × 0.45
space group (No.)	$P\bar{1}$ (2)	$P\bar{1}$ (2)
a, Å	13.415(3)	12.201(3)
b, Å	17.107(4)	12.209(3)
c, Å	13.246(3)	19.455(5)
α, deg	96.15(1)	85.34(2)
β, deg	117.45(1)	85.63(2)
γ, deg	88.06(1)	76.58(2)
V, Å^3	2681.6	2804.7
Z	2	2
D_{calc}, g/cm^3	1.693	1.661
$F(000)$	1316	1388
μ, mm^{-1}	6.02	5.78
transm coeff	0.245/0.759	0.593/0.985
R, wR^a	0.046, 0.040	
$R1$, w$R2^b$		0.052, 0.101

[a] For all structures MoKα radiation was used at $T = 296$ K. SHELXTL-Plus; $w = 1/\sigma^2(F) + 0.00001F^2$, $R = \sum||F_o| - |F_c||/\sum|F_o|$, w$R = (\sum w(|F_o| - |F_c|)^2/\sum wF_o^2)^{1/2}$. [b] SHELXL-93; $R1 = \sum||F_o| - |F_c||/\sum|F_o|$, w$R2 = (\Sigma(w(F_o2 - F_c2)^2)/\Sigma(w(F_o2)^2))^{1/2}$.

Table 3. Selected Atomic Coordinates (×10^4) and Equivalent Isotropic Displacement Parameters (Å^2 × 10^3) for $Mn_2(AuPPh_3)_2(\mu_4\text{-}PCy)(CO)_8$

	x	y	z	U(eq)[a]
Au(1)	4429(1)	2451(1)	897(1)	49(1)
Au(2)	3814(1)	2616(1)	2749(1)	47(1)
Mn(1)	7228(2)	2358(1)	3528(2)	61(1)
Mn(2)	5884(1)	2689(1)	4666(2)	54(1)
P(1)	5543(2)	3010(2)	2803(3)	44(2)
P(2)	3687(3)	1939(2)	−987(3)	51(2)
P(3)	2025(2)	2286(2)	2399(3)	47(2)
C(1)	6459(11)	1433(10)	2812(14)	75(11)
O(1)	6008(9)	852(6)	2363(11)	93(9)
C(2)	8371(13)	1828(10)	4531(15)	88(13)
O(2)	9137(10)	1504(9)	5201(12)	131(12)
C(3)	7638(11)	2366(9)	2403(14)	74(11)
O(3)	7891(9)	2374(7)	1699(10)	115(10)
C(4)	7951(10)	3304(10)	4227(14)	74(11)
O(4)	8429(8)	3893(7)	4637(10)	99(9)
C(5)	5618(12)	1588(11)	4378(13)	70(11)
O(5)	5449(10)	933(7)	4286(12)	110(10)
C(6)	4900(11)	2741(9)	5287(11)	64(10)
O(6)	4362(8)	2758(7)	5761(8)	101(9)
C(7)	6159(11)	3758(10)	5114(12)	69(10)
O(7)	6306(10)	4401(8)	5440(10)	105(10)
C(8)	7199(13)	2495(11)	5870(15)	98(14)
O(8)	8001(10)	2400(10)	6705(11)	129(13)
C(11)	5595(10)	4075(7)	2683(10)	54(8)

[a] Equivalent isotropic U defined as one-third of the trace of the orthogonalized U_{ij} tensor.

μ_3/μ_4-bridged isomers reaches the very high value of 87/13 even in the strongly polar DMSO.

Structural Descriptions. Cluster Complex 2. The chiral compound **2** crystallizes in space group $P\bar{1}$, so both of the enantiomers are present. The molecular structure (Figure 3) has a strongly distorted square pyramidal $Au_2Mn_2(\mu_4\text{-P})$ atom arrangement. As a typical structure feature of a μ_4-P atom, the heterometallic core is planar. The peculiarity of the core is an opened (Mn1···Au1 = 3.780(2) Å) as well as a closed heterometallic edge (Mn2−Au2 = 2.762(2) Å) in opposite positions. Consequently, the coordination numbers (c.n.) of the same metal atoms are different. The c.n. of the Mn(1) atom is 6 and that of the Mn(2) 7 whereas those of the gold(I) atoms are 3 for the Au(1) and 4 for the Au(2) atom. Each c.n. comprises nonmetal and metal ligand atoms. As it is known from the ligand field theory, strong energetical separation effects on the frontier orbitals of the transition metals originate in the number, kind, and the geometrical arrangement of the nonmetal ligand atoms. In the present case each manganese is bonded to four carbonyl ligands with idealized C_{2v} symmetry and to the common μ_4-P atom which reduces the symmetry of the nonmetal ligand atom geometry to C_s. If a Mn−Au bond vector is added to the opened Au(1)Mn(1) edge to attain equivalent Au−Mn edges in **2**, the deciding nonmetal coordination sphere undergoes no perturbation with respect to C_s symmetry, but there are changes of bond angles. The Au(1)−P(1)−Mn(1) bond angle (Table 5) is connected with the largest value of 35.8(1)°. This means that dissolved **2** has only a small activation energy barrier to even out both Mn−Au edges through a topomerization effect. The related fluxional behavior of the Mn−Au bonds must be triggered by an electronic imbalance for the same metal atoms which can be derived from their c.n.'s. Otherwise, from the viewpoint of the rare gas rule, the trigger seems to be at least an electron deficient Mn(1) atom in **2**. Such a property could be present in the observed Mn−Mn bond length of 2.846(4) Å which is shorter than the σ bond length of 2.943(3) Å in **1**[13] and longer than the π bond length of 2.743(3) Å in $Mn_2(\mu\text{-}PPh_2)(AuPPh_3)_3(CO)_6$.[3] It may be therefore not unreasonable to suggest a partial π delocalization effect for the Mn−Mn bond to diminish different electronic densities. Of the remaining metal−metal bonds in **2**, the Mn−Au bond is consistent with other reported σ bond lengths,[3,18] but the Au−Au bond length of 2.912(2) Å is elongated compared to that of 2.713(1) Å in $Mn_2(AuPPh_3)_2(\mu\text{-}PPh_2)(\mu\text{-}C(Ph)O)(CO)_6$.[3]

Table 4. Selected Bond Lengths (Å) and Angles (deg) for $Mn_2(AuPPh_3)_2(\mu_4\text{-}PCy)(CO)_8$

Au(1)−Au(2)	2.912 (1)	Au(1)−P(1)	2.372 (3)
Au(1)−P(2)	2.298 (3)	Au(2)−Mn(2)	2.762 (2)
Au(2)−P(1)	2.405 (2)	Au(2)−P(3)	2.303 (2)
Mn(1)−Mn(2)	2.846 (2)	Mn(1)−P(1)	2.310 (3)
Mn(2)−P(1)	2.415 (3)	P(1)−C(11)	1.852 (11)
Au(2)−Au(1)−P(1)	53.0(1)	Au(2)−Au(1)−P(2)	139.0(1)
P(1)−Au(1)−P(2)	167.9(1)	Au(1)−Au(2)−Mn(2)	102.3(1)
Au(1)−Au(2)−P(1)	51.9(1)	Au(1)−Au(2)−P(3)	120.2(1)
Mn(2)−Au(2)−P(1)	55.2(1)	Mn(2)−Au(2)−P(3)	133.9(1)
P(1)−Au(2)−P(3)	170.8(1)	Mn(2)−Mn(1)−P(1)	54.7(1)
Au(2)−Mn(2)−Mn(1)	97.7(1)	Au(2)−Mn(2)−P(1)	54.9(1)
Mn(1)−Mn(2)−P(1)	51.3(1)	Au(1)−P(1)−Au(2)	75.1(1)
Au(1)−P(1)−Mn(1)	107.7(1)	Au(1)−P(1)−Mn(2)	134.8(1)
Au(2)−P(1)−Mn(1)	127.2(1)	Au(2)−P(1)−Mn(2)	69.9(1)
Au(2)−P(1)−C(11)	112.3(3)	Mn(1)−P(1)−Mn(2)	74.1(1)
Mn(1)−P(1)−C(11)	117.3(3)	Mn(2)−P(1)−C(11)	114.7(4)

(18) Iggo, J. A.; Mays, M. J.; Raithby, P. R.; Henrick, K. *J. Chem. Soc., Dalton Trans.* **1984**, 633.

Table 5. Selected Atomic Coordinates ($\times 10^4$) and Equivalent Isotropic Displacement Parameters (Å $\times$ 10^3) for $Mn_2(\mu$-AuPCy$_3)(\mu_3$-PCy(AuPCy$_3$))$(CO)_8$

	x	y	z	U(eq)[a]
Au(1)	5343(1)	2370(1)	1292(1)	38(1)
Au(2)	2941(1)	−79(1)	3166(1)	40(1)
Mn(1)	4396(1)	2370(1)	2607(1)	38(1)
Mn(2)	3334(1)	1806(1)	1356(1)	37(1)
P(1)	7049(2)	2368(2)	670(1)	36(1)
P(2)	2815(2)	1638(2)	2525(1)	33(1)
P(3)	3186(2)	−1669(2)	3924(1)	40(1)
C(1)	4245(7)	2322(8)	3521(5)	55(2)
O(1)	4147(6)	2315(6)	4120(3)	83(2)
C(2)	5276(7)	918(8)	2622(4)	47(2)
O(2)	5846(6)	26(6)	2669(3)	72(2)
C(3)	5660(8)	2963(9)	2559(5)	64(3)
O(3)	6408(6)	3351(7)	2609(4)	103(3)
C(4)	3518(8)	3805(8)	2570(4)	51(2)
O(4)	2983(7)	4684(6)	2618(4)	90(3)
C(5)	2639(7)	3311(8)	1279(4)	47(2)
O(5)	2209(6)	4243(6)	1203(4)	85(2)
C(6)	4174(7)	362(8)	1437(4)	46(2)
O(6)	4697(6)	−560(6)	1471(4)	74(2)
C(7)	2111(7)	1382(7)	1136(4)	48(2)
O(7)	1327(5)	1114(6)	962(3)	70(2)
C(8)	3856(8)	1930(9)	466(5)	66(3)
O(8)	4080(6)	1973(8)	−122(4)	104(3)

[a] Equivalent isotropic U defined as one-third of the trace of the orthogonalized U_{ij} tensor.

Table 6. Selected Bond Lengths (Å) and Angles (deg) for $Mn_2(\mu$-AuPCy$_3)(\mu_3$-PCy(AuPCy$_3$))$(CO)_8$

Au(1)−P(1)	2.326(2)	Au(1)−Mn(2)	2.6880(13)
Au(1)−Mn(1)	2.7263(14)	Au(2)−P(3)	2.317(2)
Au(2)−P(2)	2.330(2)	Mn(1)−P(2)	2.327(2)
Mn(1)−Mn(2)	3.041(2)	Mn(2)−P(2)	2.318(2)
P(1)−Au(1)−Mn(2)	147.47(6)	C(8)−Au(1)−Mn(2)	39.3(2)
Mn(2)−Au(1)−Mn(1)	68.34(4)	C(3)−Au(1)−Mn(1)	39.7(2)
P(3)−Au(2)−P(2)	171.49(8)	P(2)−Mn(1)−Au(1)	103.76(7)
P(2)−Mn(1)−Mn(2)	48.98(6)	Au(1)−Mn(1)−Mn(2)	55.23(3)
P(2)−Mn(2)−Au(1)	105.20(7)	P(2)−Mn(2)−Mn(1)	49.24(6)
Au(1)−Mn(2)−Mn(1)	56.43(4)	Mn(2)−P(2)−Mn(1)	81.78(8)
Mn(2)−P(2)−Au(2)	124.07(9)	Mn(1)−P(2)−Au(2)	112.06(9)

Cluster Complex 5. The molecular structure of the diamagnetic title compound (Figure 7) can be derived from **1**, an edge-sharing coordination bioctahedron,[13] through the substitution of both the hydrogen atoms by the corresponding number of $AuPCy_3$ residues. Orthogonal to the common edge which is formed by the groups μ-$AuPCy_3$ and μ_3-PCy($AuPCy_3$) exists the Mn−Mn bond vector of 3.041(2) Å in the 34 valence electrons (VE) complex. As compared to dimanganese complexes with this VE number, this bond length is longer than that of 2.940(1) Å in **1** but distinctly shorter than that of 3.130(2) Å in $Mn_2(\mu$-AuPPh$_3)(\mu$-PCyH$)(CO)_8$.[16] The last-named alteration indicates that the origin is mainly electronic. The substitution of the group $AuPPh_3$ (−M effect of Ph) by $AuPCy_3$ (+I effect of Cy) in the studied compounds makes the gold(I) atom more electron rich and leads to Mn−Mn bond strengthening. On the basis of the same reason, the previously mentioned elongation of the Mn−Mn bond length corresponds to an increase of an electron-withdrawing effect on the way from hydrogen in **1** to two $AuPCy_3$ residues in **5** as substituents. The other structural features are typical of such dimanganese complexes and need no further comment.

Conclusions

The transformation described in this work comprises an isomerization process between μ_3-P- and μ_4-P-bridged pairs of isomers including a fluxional Mn−Au bond in the μ_4-isomer (topomerization process). The isomerization process depends on the kind of phosphine attached to gold(I) which can be controlled by electronic and/or steric factors and additionally by the polarity of the solvent used. This observed sensitivity led us to the idea of studying the mechanistical pathway of formation of such dimanganese complexes and to look for a parallel chemical behavior with the homologous dirhenium complex $Re_2(\mu$-H$)(\mu$-PCyH$)(CO)_8$ instead of **1** as starting material. To underline the peculiarity of the dimanganese reaction system studied it is interesting to know that under analogous reaction conditions the above dirhenium compound only leads to the isomer $Re_2(\mu$-AuPPh$_3)(\mu_3$-PCy($AuPPh_3$))$(CO)_8$ as the unique product. This compound corresponds to **3** which is not the thermodynamically preferred isomer in the dimanganese reaction systems.[19] This means that only **3** and related dimanganese isomers are able to isomerize under the given reaction conditions. The rearrangement from **3** to **2** is accompanied by a loss of a Mn−Au bond in **2** which is compensated for by additional Au−P and Au−Au bonds in **3**. In the case of the dirhenium compound the rearrangement does not take place because of a Re−Au bond being usually stronger than a Mn−Au bond.

The isomerization processes of the related manganese compounds $Mn_2(\mu$-AuPR$_3)(\mu$-PCyH$)(CO)_8$/$Mn_2(\mu$-H$)(\mu$-PCy(AuPR$_3$))$(CO)_8$ (R = Ph, Cy, p-C_6H_4F, p-C_6H_4OMe) including kinetic studies[16] and the reactivity of the mentioned dirhenium complex[19] will be considered in further papers.

Supplementary Material Available: Listings of complete atomic coordinates and U values, bond distances and angles, anisotropic displacement parameters, and hydrogen atom coordinates for **2** and **5** (13 pages). Ordering information is given on any current masthead page.

IC940470S

(19) Haupt, H.-J.; Schwefer, M.; Flörke, U. Z. *Anorg. Allg. Chem.*, in press.